16th World Conference on Earthquake, 16WCEE 2017
Santiago Chile, January 9th to 13th 2017
Paper N° 726
Registration Code: S-K1461628893

Study on Seismic Response in Substation Steel Structures

D. Takabatake[(1)], S. Nagata[(2)], T. Kobayashi[(3)], H. Nakakoji[(4)], Y. Katou[(5)] and S. Iwasaki[(6)]

[(1)] *Central Research Institute of Electric Power Company, tdaisuke@criepi.denken.or.jp*
[(2)] *Central Research Institute of Electric Power Company, n-seiji@criepi.denken.or.jp*
[(3)] *Tokyo Electric Power Co., Inc., KOBAYASHI.TAKAYUKI@tepco.co.jp*
[(4)] *Tokyo Electric Power Co., Inc., nakakoji.hajime@tepco.co.jp*
[(5)] *Chubu Electric Power Co., Inc., Katou.Yoshihiro2@chuden.co.jp*
[(6)] *The Kansai Electric Power Co., Inc., iwasaki.shinya@d5.kepco.co.jp*

Abstract

After the 2011 off the Pacific coast of Tohoku Earthquake in Japan (M9.0), it was found that the damage ratio of substation equipment was less than 1% at the substations experiencing strong ground motion with a peak ground acceleration of over 300gal. Consequently, the seismic performance of the existing substation equipment has been demonstrated. However, the steel frame structures of a substation are designed with consideration of the wind load mainly. Furthermore, there have been only few researches related to the seismic response of the steel frame. These backgrounds make difficult to establish the precise technique in seismic performance evaluation. Therefore, this paper presents the fundamental seismic response and the numerical simulation on a steel frame. The target steel frame is a two-dimensional frame structure connected to other equipment with conductors in the out-of-plane direction. To verify an analytical idealization for the seismic performance evaluation of the steel frame, a seismic observation during its operation and a dynamic numerical analysis using the finite element method were performed. In the numerical model, three models with different conditions in idealization of the conductors were generated. In one model, the conductors are not modeled. In the other two models, the conductors are modeled by point mass elements or by beam elements. We examined the effects of the conductors on the dynamic characteristics, such as natural frequency and mode shape, and the seismic response, such as the displacement of the steel frame and stresses of the structural members. Based on these results, it was found that the dynamic characteristics of the steel frame in the direction normal to the conductors were less affected by the conductors. On the other hand, the dynamic characteristics in the direction parallel to the conductors were complicated owing to the effect of the conductors. Because the stresses in the structural members during the earthquake were also affected by the conductors, a detailed model of the conductors was needed in the numerical analysis in order to obtain the reasonable evaluation.

Keywords: Substation, Steel structures, Conductors, Structural analysis, Seismic Response

1. Introduction

It has been found that a damage ratio of substation equipment due to the 2011 off the Pacific Coast of Tohoku Earthquake (M9.0) was less than 1% in the regions where the maximum ground acceleration exceeded 300gal. This damage ratio is small enough to recognize that the substation equipment in Japan would perform well during large earthquakes assumed in the near future. However, we should pay more attention to the fact that there have been few researches in both experimental and analytical approaches, therefore little is known about the seismic response and the seismic resistance in the substation equipment. This is because even though steel frame structures of substations, for instance, have been designed with consideration of the wind load mainly [1][2], as a result this design procedure have given a certain design margin in the seismic performance. However, to obtain a realistic estimation for the damage ratio in the event of large earthquakes, the fundamental seismic performance in the steel frames should be carefully investigated for establishment of the precise technique in seismic performance evaluation [3].

From the background described above, we have carried out a seismic observation on a steel frame during its operation in order to clarify the realistic seismic response. Since the verification of the numerical model is one of the most important issues in the establishment of the precise technique, a series of numerical simulations

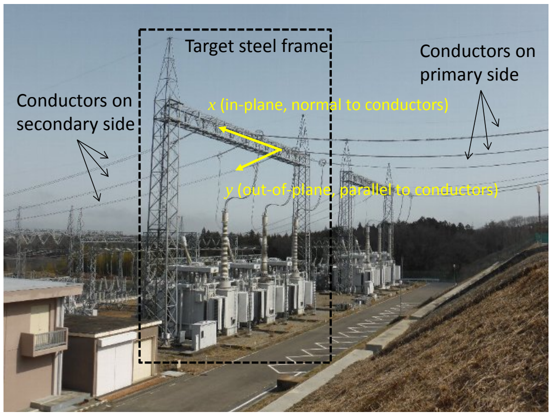

Fig. 1– Appearance of the target steel frame structure

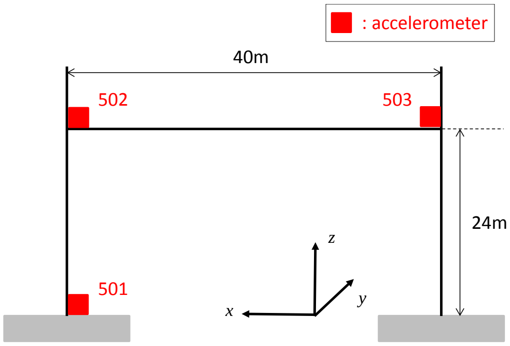

Fig. 2 – Configuration and layout of the accelerometers in the steel frame

were performed in this research, and also analytical correlations were confirmed based on the observation data. The steel frames of substation are typically connected to the other substation equipment with the conductors. Thus three numerical models with different conditions in modeling of the conductor were generated by using the finite element method. First, the eigenvalue analysis was performed to determine the natural mode shapes and the natural frequencies of the steel frame. Then the dynamic numerical analysis in which the ground acceleration data was used as an input motion was performed to estimate the damping ratio in the steel frame. To evaluate the effect of the conductors on the accuracy of the numerical simulations, not only the response in the whole structure but also the stresses developed in the structural members during the earthquake were discussed.

2. Target Frame and Methods

2.1 Target steel frame structure and seismic observation method

In this paper, the steel frame structure of a substation was targeted to analyze the dynamic characteristics by seismic observation and numerical analysis. The target steel frame is shown in Fig.1, which is a two-dimensional steel frame with a post height of 24m and a beam length of 40m that is connected to flexible conductors with insulators. In this paper, the coordinate system is defined with the *x*-direction parallel to the conductors, the *y*-direction normal to the conductors, and the *z*-direction in the vertical direction. The steel frame consists of angle members made of SS400 steel ranging in size from L130×9 to L45×4. The total mass of the steel frame is 22.3ton. On the primary side, three 1260mm^2 hard drawn aluminum conductors are connected. The unit mass of one conductor is 0.0315kg/m and its span length, difference in height, sag, and the line angle between the steel frame and the contiguous structure are 61.3m, -8.5m, 3.2%, and 24°, respectively. The insulator used on the primary side is a 500kV long rod insulator string for three conductors, whose mass is 0.4ton. On the secondary side, two 660mm^2 heat-resistant aluminum alloy conductors are connected. The unit mass of one conductor is 0.0111kg/m and its span length, difference in height, sag, and the line angle between the steel frame and the contiguous structure are 66.7m, +11.6m, 2.2%, and 14°, respectively. The insulator used on the secondary side is a 275kV long rod insulator string for two wires, whose mass is 0.15ton.

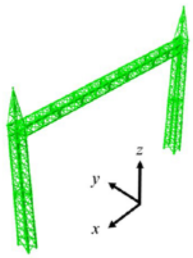

(a) Steel frame without conductors (model A)

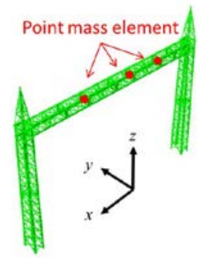

(b) Steel frame with point mass element(model B)

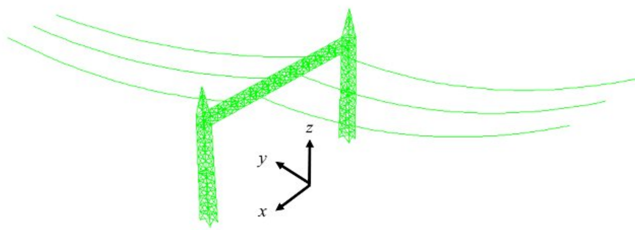

(c) Steel frame with conductors (model C)

Fig. 3 – Finite element models of the steel frame used in the numerical analysis

Fig.2 shows the configuration of the steel frame and the layout of the accelerometers used in the seismic observation. The accelerations at the base of the steel frame (observation point 501) and at both ends of the beam (observation points 502 and 503) are measured using a triaxial accelerometer under the condition that the range of acceleration is 2000gal and the sampling frequency is 200Hz. The seismic observation started in August 2012 and more than 20 sets of measurements during earthquakes have been obtained.

2.2 Evaluation of dynamic characteristics of steel frame

To investigate the dynamic characteristics of the steel frame such as the natural mode, damping ratio, and seismic response, not only seismic observation but also numerical analysis was carried out. First, to calculate the natural frequency and natural mode shape of the steel frame with conductors, eigenvalue analysis using the finite element method was performed. Three FE models were generated to clarify the effect of the conductors on the natural mode, as shown in Fig.3. In this study, the commercial FE program ABAQUS[4] was used for the numerical analysis. In model A, the steel frame is modeled by two-node linear beam elements, but the conductors are not modeled as shown in Fig.3(a). In model B, the steel frame is modeled in the same way as in model A, and the conductors are modeled by point mass elements located at the insulators as shown in Fig.3(b). The magnitude of each point mass element is estimated as the sum of the insulator mass and half of the total mass of the conductors. In model C, the steel frame is modeled in the same way as in models A and B, and the conductors are also modeled by two-node linear beam elements as shown in Fig.3(c). Note that the contiguous structures are not modeled and the only heights of the insulators in the contiguous structures are considered. In the eigenvalue analysis, the relationship between the natural frequency and the effective mass ratio was also focused on to identify the dominant natural mode.

Next, to investigate the basic seismic response of the steel frame during earthquakes, the maximum accelerations and the transfer functions were calculated using the data obtained by seismic observation. Here, the maximum accelerations and the Fourier amplitude spectrum of the acceleration were calculated at each observation point. The transfer function was also calculated by dividing the Fourier amplitude spectrum at both ends of the beam by that at the base.

To estimate the damping ratio of the steel frame, dynamic numerical analysis in time domain was also performed. In this numerical analysis, the Hilber-Hughes-Taylor method (HHT) [4] was used as the time integration technique and the parameter α in HHT was set to 0.05. The numerical analysis using FE model A was performed to determine the damping ratio of the steel frame without the conductors. The damping ratio of the steel frame was set to 1%, 2%, 3%, 5%, and 10%, then the seismic response was calculated using the proportional stiffness damping model based on the first natural frequency for each damping ratio. In these calculations, the triaxial acceleration recorded at the base of the steel frame during an earthquake was used. Finally, comparing the transfer functions obtained by observation with that obtained by numerical analysis, the optimum value for the damping ratio was determined, which led to good agreement between the transfer functions obtained by observation and numerical analysis.

In addition, to examine the effect of the conductors on the accuracy of the numerical results, we compared the numerical results obtained using models A and C. Here, the seismic response was calculated by dynamic numerical analysis as mentioned above. In these calculations, the damping ratio of the steel frame was set on the basis of the results of the analysis in this paper. On the other hand, the damping ratio of the conductors was set to 0.4%. To evaluate the accuracy of the numerical results, we compared the seismic responses, such as the maximum displacement, acceleration, and transfer function, between the observed and numerical results. Furthermore, using these numerical results, we also investigated the effect of the conductors on the member stress during earthquakes.

3. Results

3.1 Natural frequency and natural mode shape

The eigenvalue analysis using the three FE models was performed to investigate the natural frequencies and natural mode shapes. The first natural frequencies and the natural mode shapes in the *x*- and the *y*-directions obtained by eigenvalue analysis are shown for models A – C in Figs.4-6, respectively. In these figures, the mode shapes are shown in both the *xz*-plane (in-plane) and the *yz*-plane (out-of-plane). In addition, the relationship between the natural frequency and the effective mass ratio is also shown in these figures.

In model A, the first natural frequency in the *x*-direction was 1.68Hz and the two posts bent in the in-plane in the same direction as shown in Fig.4(a). On the other hand, the first natural frequency in the *y*-direction was 1.52Hz and the two posts bent out of the plane in the same direction as shown in Fig.4(b). Because the effective mass ratios of the first natural mode in the *x*- and the *y*-direction were 82.3% and 74.3%, respectively, as shown in Fig.4(c), the first natural modes in each direction were dominant in model A.

In model B, the first natural frequency in the *x*-direction was 1.40Hz and the two posts bent in the in-plane in the same direction as shown in Fig.5(a). On the other hand, the first natural frequency in the *y*-direction was 1.21Hz and the two posts bent out of the plane in the same direction as shown in Fig.5(b). Because the effective mass ratios of the first natural mode in the *x*- and the *y*-direction were 86.3% and 79.0%, respectively, as shown in Fig.5(c), the first natural modes in each direction were dominant in model B. Whereas the natural mode shapes in model B were similar to those in model A and the same natural modes were dominant, the natural frequencies in model B were smaller than those in model A.

In model C, the first natural frequency in the *x*-direction was 1.61Hz and the two posts bent not only in the in-plane direction but also in the out-of-plane direction as shown in Fig.6(a). On the other hand, the first natural frequency in the *y*-direction was 0.91Hz and the displacement of the conductors was greater than that of the steel frame as shown in Fig.6(b). Furthermore, there were numerous natural modes over a wide frequency range in which the displacement of the conductors was dominant as shown in Fig.6(c).

3.2 Seismic response during earthquakes

The maximum acceleration and the transfer function were calculated using the data obtained by seismic observation. Fig.7 shows time histories of the acceleration at the base of the steel frame and Fig.8 shows the acceleration response spectra for a damping ratio of 1.0% obtained using time histories shown in Fig.7. The specifications of the earthquake were as follows: the magnitude was 7.3, the focal depth was 49km, and the distance from the epicenter was 303km. The maximum accelerations at the base of the streel frame during the earthquake were 66.2gal in the *x*-direction, 82.1gal in the *y*-direction, and 57.7gal in the *z*-direction. Subsequently, we focused on the response of the beam during the earthquake. The maximum accelerations at

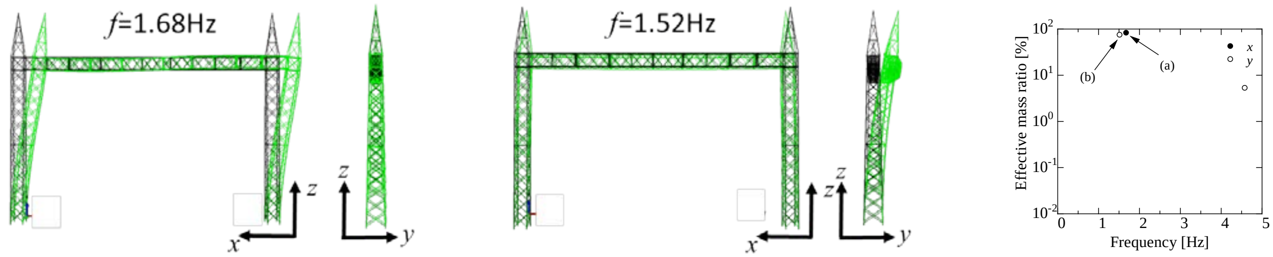

(a) Natural mode in the *x*-direction (b) Natural mode in the *y*-direction (c) Natural frequency

Fig. 4 – Natural mode shape and natural frequency based on model A

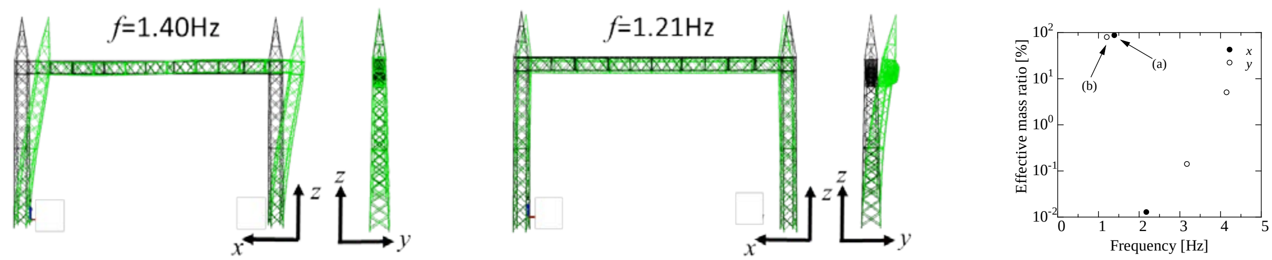

(a) Natural mode in the *x*-direction (b) Natural mode in the *y*-direction (c) Natural frequency

Fig. 5 – Natural mode shape and natural frequency based on model B

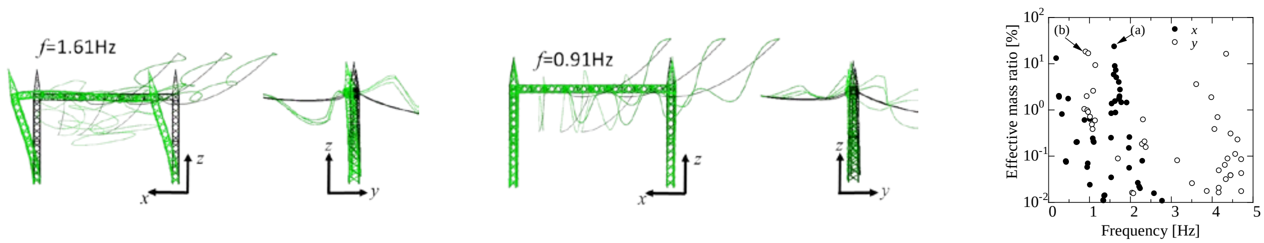

(a) Natural mode in the *x*-direction (b) Natural mode in the *y*-direction (c) Natural frequency

Fig. 6 – Natural mode shape and natural frequency based on model C

observation point 502, which is directly above observation point 501 on the base, were 107.9gal in the *x*-direction, 135.4gal in the *y*-direction, and 110.0gal in the *z*-direction.

The transfer functions in the *x*-and *y*-directions obtained by observation at observation points 502 and 503 are shown in Figs.9(a) and 9(b), respectively. The closed triangles show the resonance peaks appearing in both transfer functions. The transfer functions at the two observation points are in good agreement, particularly in the *x*-direction. In the *x*-direction, there was a clear dominant peak at a frequency of 1.65Hz. On the other hand, the transfer function in the *y*-direction was so complicated that it was difficult to identify a clear dominant peak. The peak at a frequency of 1.67Hz was the dominant peak in the *y*-direction because its amplitude ratio was the largest.

3.3 Damping ratio of the steel frame

The damping ratio of the streel structure was estimated by comparing the transfer functions obtained by observation and numerical analysis. Here, the transfer functions in the *x*-direction were used because the seismic response in the *x*-direction could be assumed to be less affected by the conductor as discussed later. The transfer functions are compared in Fig.10. The greater the damping ratio, the lower the amplitude ratio of the peak in the transfer functions obtained by numerical analysis. The transfer function obtained by numerical analysis for a

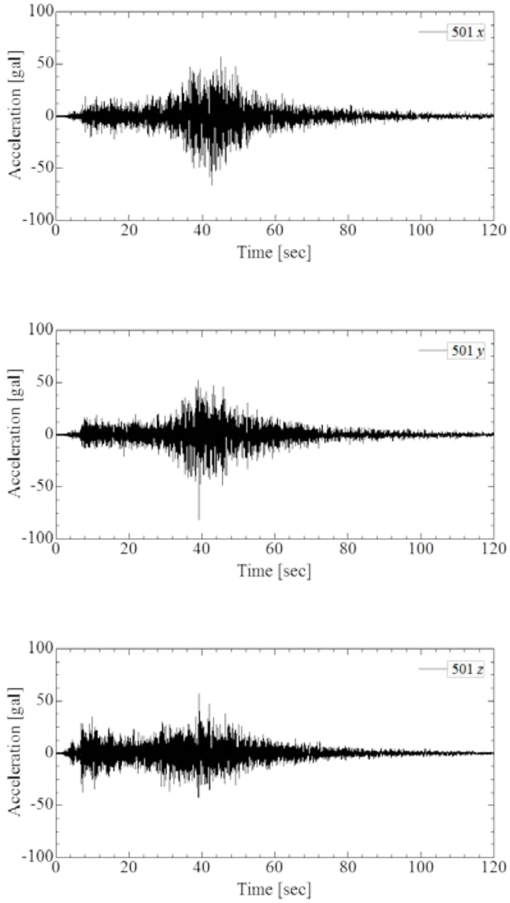

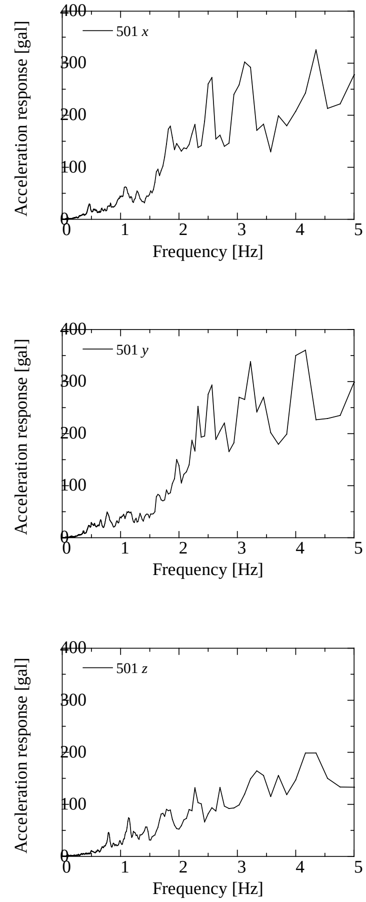

Fig. 7 –Time histories of acceleraion at the base Fig. 8 – Acceleration response spectra (h=1%)

damping ratio of 1% was in good agreement with that obtained by observation. Furthermore, this result is also in agreement with the damping ratio of general steel structures [5]. Thus, the damping ratio of the steel frame without conductors was estimated to be 1%.

3.4 Effect of the conductors on the accuracy of the numerical results

On the basis of the results of the time history dynamic numerical analysis using FE models A and C, the effect of the conductors on the accuracy of the numerical results was investigated. First, the transfer functions obtained by numerical analysis and observation were compared as shown in Fig.11. Fig.11(a) shows the transfer functions in the *x*-direction at observation point 502, and Fig.11(b) shows those in the *y*-direction at the same point. In the *x*-direction, both transfer functions obtained by numerical analysis were in good agreement with that obtained by observation. On the other hand, in the *y*-direction, the resonance frequency of the main peak based on the numerical results using model A was different from that based on the observation. In addition, the numerical results using the model A did not reproduce the small resonance peaks in the transfer function obtained by observation. However, the resonance frequency of the main peak based on the numerical results using model C was in good agreement with that based on the observed result. Furthermore, the numerical results using the model C also reproduce the small resonance peaks in the transfer function obtained by observation.

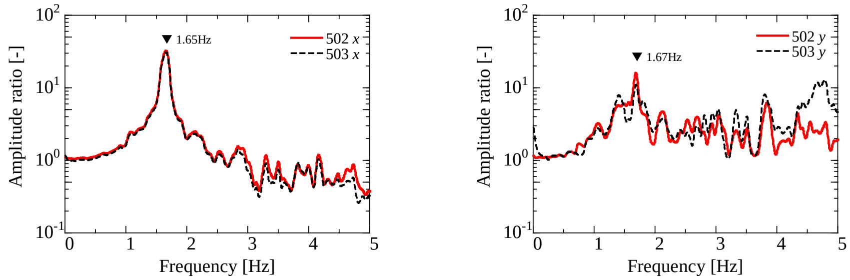

(a) *x*-direction (b) *y*-direction

Fig. 9 – Amplitude ratios

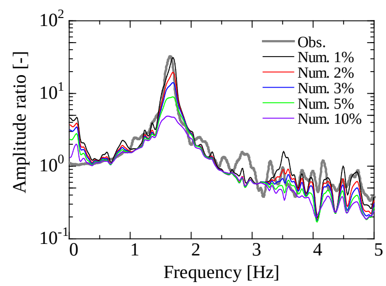

Fig. 10 – Comparison of transfer functions

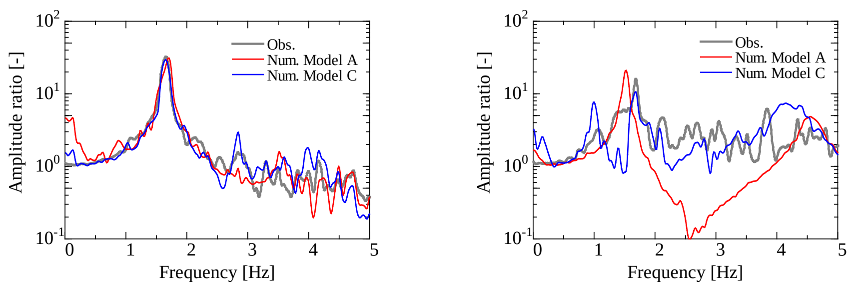

(a) *x*-direction (b) *y*-direction

Fig. 11 – Amplitude ratios

Table 1 shows the maximum displacement and acceleration at observation point 502 obtained from the numerical results using FE models A and C, and those based on the observed results. Here, the displacement based on the observed results was calculated by integrating the time history of the acceleration twice. In the *x*-direction, both the maximum displacement and the acceleration based on the numerical results were in good agreement with those based on the observed results. On the other hand, in the *y*-direction, both the maximum displacement and the acceleration based on the numerical results were smaller than those based on the observed results. However, comparing the numerical results obtained using models A and C, the maximum displacement and acceleration using model C were closer to the observed results than those using model A.

3.5 Effect of the conductors on the member stress

The member stress was obtained by numerical analysis using models A and C. In this paper, to evaluate the member stress, we divided the post into 16 blocks, and members were also divided into main leg members and bracing members. Furthermore, bracing members were distinguished by their location, *x*-direction bracing members which were in the plane, and *y*-direction bracing members which were out of the plane as shown in

Table 1 – Peak response obtained by analysis

		Acceleration [gal]	Displacement [cm]
Model A Without conductors	*x* (Num./Obs.)	91.4 (0.85)	0.79 (0.92)
	y (Num./Obs.)	63.7 (0.47)	0.38 (0.54)
Model C With conductors	*x* (Num./Obs.)	87.1 (0.81)	0.93 (1.08)
	y (Num./Obs.)	115.8 (0.86)	0.46 (0.65)
Observation	*x*	107.9	0.86
	y	135.4	0.71

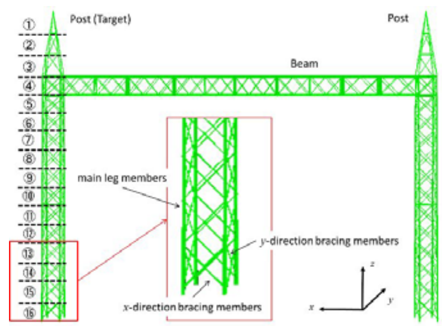

Fig. 12 – Definition of members

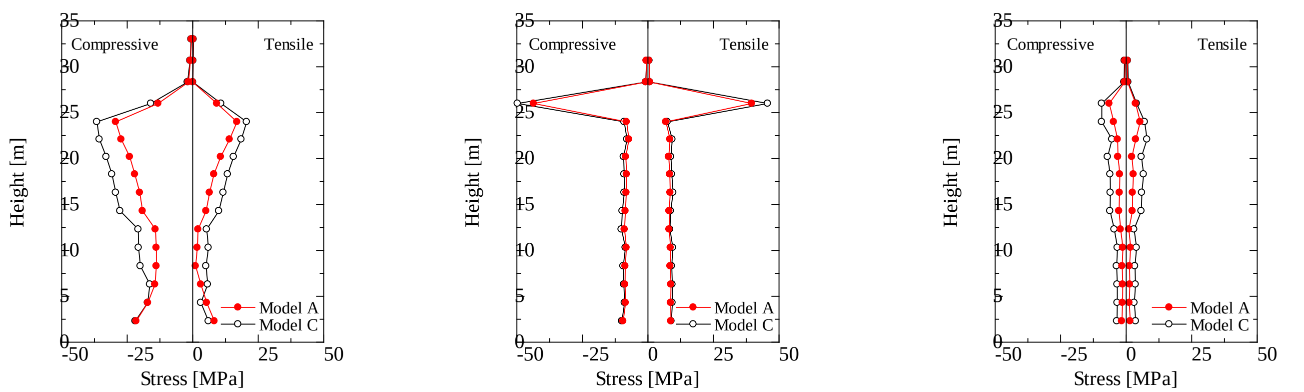

(a) Main leg members (b) *x*-direction bracing members (c) *y*-direction bracing members

Fig. 13 – Maximum stress distributions

Fig.12. The height-direction distributions of the maximum member stress obtained by numerical analysis are shown for main leg members in Fig.13(a), for *x*-direction bracing members in Fig.13(b), and for *y*-direction bracing members in Fig.13(c). In these figures, positive stress corresponds to tensile stress and negative stress corresponds to compressive stress. In the main leg members, whereas the compressive stress was larger than the tensile stress, both distributions were similar. Both the tensile stress and the compressive stress increased from the bottom to the top and had a peak at the block under the joint block (No.4 as shown in Fig.12) connecting the beam and the post. This was because the bending moment around the *y*-direction was concentrated around joint block. Furthermore, both stresses in model C were larger than those in model A. In the *x*-direction bracing members, both the tensile stress and the compressive stress had a peak at the joint block connecting the beam and the post, and both stresses were almost constant below the joint block. This was also because the bending

moment around the *y*-direction was concentrated around joint block. Furthermore, both stress distributions in model C were almost the same in those in model A. In the *y*-direction bracing members, both the tensile stress and the compressive stress slightly increased from the bottom to the top and had a peak at the block under the joint block. Furthermore, both stresses in model C were larger than those in model A.

4. Discussion

4.1 Natural mode of the steel frame

To investigate the natural frequency and natural mode shape, not only seismic observation but also numerical analysis using the finite element method was carried out. In the analysis, to clarify the effect of the conductors on the natural mode, three FE models were generated. Comparing the natural mode in the *x*-direction between models A and C, as shown in Figs.4(a) and 6.(a), whereas the mode shapes out of the plane were different, the mode shapes as well as the natural frequencies in the plane were almost the same. Furthermore, the transfer function was also almost the same for both models, as shown in Fig.11(a). Thus, it was found that the dynamic characteristics of the steel frame in the *x*-direction, namely, the direction normal to the conductors, were less affected by the conductors.

Comparing the natural mode in the *y*-direction between in models A and C, as shown in Figs.4(b) and 6(b), although the post bent in the out-of-plane direction in model A, the steel frame was not displaced whereas the conductors were displaced in model C. Furthermore, comparing the transfer functions between models A and C, as shown in Fig.11(b), although there was a clear dominant peak in the transfer function for model A, there was not dominant peak and a number of small peaks in the transfer function for model C. Thus, it was found that the dynamic characteristics of the steel frame in the *y*-direction, namely, the direction parallel to the conductors, was so complicated that a number of natural modes associated with the conductors were generated owing to the fluctuating tension of the conductors. These behaviors are also consistent with the response of an overhead transmission tower in the parallel direction to the conductors being more complicated than that in the normal direction to the conductors [6].

4.2 Methods used to model the conductors

When the seismic response of a steel frame is estimated by numerical simulation, it is necessary to model the conductors because the natural mode is affected by the conductors as mentioned above. In this paper, two methods were used to model the conductors: using point mass elements (model B), and using beam elements (model C). In model C, not only the dominant natural frequency but also the transfer function was in agreement with those based the seismic observation in the *x*-direction, as shown in Fig.11(a). On the other hand, in the *y*-direction, whereas the transfer function did not completely coincide with that based on seismic observation, the numerical result reproduced the effect of the conductors of generating a number of natural modes. Furthermore, the seismic responses, such as the maximum acceleration and displacement, calculated using model C were in agreement with those based on seismic observation as shown in Table 1. On the other hand, for model B, although the shape of the first natural mode in the *x*-direction was similar to that for model C, the first natural frequency in the *x*-direction and the dynamic characteristics in the *y*-direction were different from those for model C. Thus, it was found that the method using point mass elements for the conductors did not reproduce the seismic response of the steel frame with the conductors, making it necessary to use the beam elements for the conductors.

5. Conclusion

In this study, for the verification of the numerical models for a steel frame structure of a substation, a seismic observation during its operation as well as a dynamic numerical analysis based on the finite element method was performed. The dynamic characteristics such as the natural mode shape, natural frequency and damping ratio were first determined and then the effect of the conductors on the seismic response was evaluated.

As a result, when the conductors were modeled by the beam elements, the natural mode shapes in the *y*-direction, which was parallel to the conductors, was complicated and the number of natural modes increased. This was because the natural modes of the steel frame were affected by the specific mode of the conductors through their tension fluctuation. The numerical model including the conductors by the beam elements gave better correlation with the seismic observation data than that ignoring the conductors. On the other hand, the seismic response in the *x*-direction, which was normal to the conductors, was also affected by the conductors, but the influence in the *x*-direction was much smaller than that in the *y*-direction. Because not only global response in the steel frame but also the stress in the structural members during the earthquake were affected by the conductors, the detailed model of the conductors was required for the numerical analysis in order to obtain the reasonable seismic performance evaluation.

References

[1] Electric Technology Research Association (1978): Henden kiki no taishin sekkei [Seismic design for substation equipment]. Electric Technology Research, **34** (3), Electric Technology Research Association

[2] The Japan Electric Association (2010): Hendensyo ni okeru denki setsubi no taishin sekkei shishin [Seismic design guide for electric equipment in substation]. JEAG 5003-2010, The Japan Electric Association

[3] Ohno I, Ito T, Nakakoji H, Kobayashi T, Sato H (2014): Study of seismic design and guideline of substation equipment based on the Great East Japan Earthquake. *Proc. CIGRE Paris International Conference*

[4] ABAQUS Analysis User's Manual Version 6.12 (2013)

[5] Architectural Institute of Japan (2000): Damping of buildings. Architectural Institute of Japan

[6] Sato Y, Ishikawa T, Takabatake D (2011): Observation study of an overhead transmission tower under operation. *Proc. Japan Association Civil Engineering Annual Conference*